

Enhancing Auditory BCI Performance: Incorporation of Connectivity Analysis

Talukdar Raian Ferdous

Department of Biomedical Engineering

University of Houston

Houston USA

tferdous@cougarnet.uh.edu

Luca Pollonini

Department of Engineering Technology

University of Houston

Houston USA

lpolloni@central.uh.edu

Joseph Thachil Francis

Department of Biomedical Engineering

University of Houston

Houston USA

jtfranci@central.uh.edu

Abstract— Brain connectivity analysis to classify auditory stimuli applicable to invasive auditory BCI technology, particularly intracranial electroencephalography (iEEG) remains an exciting frontier. This study revealed insights into brain network dynamics, improving analysis precision to distinguish related auditory stimuli such as speech and music. We thereby contribute to advancing auditory BCI systems to bridge the gap between noninvasive and invasive BCI by utilizing noninvasive BCI methodological frameworks to invasive BCI (iEEG) data. We focused on the viability of using connectivity matrices in BCI calculated across brain waves such as alpha, beta, theta, and gamma. The research highlights that the traditional machine learning classifier, Support Vector Machine (SVM), demonstrates exceptional capabilities in handling brain connectivity data, exhibiting an outstanding 97% accuracy in classifying brain states, surpassing previous relevant studies with an improvement of 9.64%. The results are significant as we show that neural activity in the gamma band provides the best classification performance using connectivity matrices calculated with Phase Locking Values and Coherence methods.

Keywords— Brain Connectivity, Neural Networks, Machine Learning, Deep Learning

I. INTRODUCTION

Brain-Computer Interface (BCI) research in differentiating between speech and music is crucial for personalized BCI development, improving user interaction, and enhancing the precision of auditory-based BCIs. Essential research aspects involve identifying the predominant influence of distinct brain waves (alpha, beta, theta, and gamma) in processing auditory information and elucidating the role of connectivity among diverse brain regions in stimulus classification. Brain connectivity analysis has advanced significantly over the years, incorporating methodological frameworks in time, frequency, and information domains and innovations in interpreting the results and visualizing connected brain regions [1]. Brain connectivity analysis, while extensively studied in noninvasive BCI studies using electroencephalography (EEG), remains an exciting open frontier when applied to invasive BCI datasets, particularly intracranial electroencephalography (iEEG) [2]. In this report, we show the potential to reveal new perspectives on brain network dynamics, facilitating analysis with increased signal-to-noise

ratio and spatial precision, which could contribute to the advancement of BCI technology. Despite advancements, the underexplored significance of brain connectivity matrices in BCI investigations remains a gap in current research, possibly limiting the decoding of relevant information from neural signals. Various machine learning and deep learning algorithms have been tested to classify different brain states using connectivity matrices. One study employed a support vector machine (SVM) classifier utilizing coherence and correlation-based connectivity features to achieve a classification accuracy of 87.04% [3]. Two-dimensional convolutional neural networks were explored with connectivity matrices calculated using Pearson correlation coefficient (PCC), phase locking value (PLV), and transfer entropy (TE) with the highest accuracy achieved, 87.36%, in the case of PLV with a kernel size of (5x5) [4]. Other tested classifiers were k-nearest neighbors and random forests, with the highest accuracy of 48.50 and 51.34%, respectively [5]. This report aims to consolidate scattered information by introducing noninvasive BCI methodologies to invasive BCI (iEEG) data. We specifically focused on illustrating the viability of connectivity matrices calculated across various frequencies, encompassing theta (4-7 Hz), alpha (8-12 Hz), beta (13-30 Hz), and gamma (31-45 Hz). Four calculation methods—phase locking value (PLV), phase lag index (PLI), coherence (COH), and pairwise phase consistency (PPC)—were utilized to discern closely related auditory stimuli, such as music and speech. For classification purposes, the study employed a Support Vector Machine (SVM), Random Forest (RF), K-Nearest Neighbor (KNN), Gaussian Process (GP), Naive Bayes (NB), 2D Convolutional Neural Network (2D-CNN), and Multilayer Layer Perceptron (MLP) classifiers.

II. METHOD

A. Dataset and Task Description

An open access iEEG dataset from open neuro database was utilized for this study, which comprises 51 participants with medication-resistant epilepsy who underwent intracranial electrode implantation at the University Medical Center Utrecht [6]. Notably, the dataset predominantly includes perisylvian grid coverage, with many patients having electrodes strategically placed in frontal and motor cortices. The tasks involved a 6.5-minute movie-watching procedure for language mapping and a three-minute resting state

*This Research was supported by NIH 1R01NS124222-01, 1R01NS125435-01A1

experiment. Developed for language mapping, the clinical task involved a movie with 13 alternating blocks of speech and music, each lasting 30s. This comprised seven blocks of music and six blocks of speech, creating a structured yet dynamic stimulus for assessing language-related neural responses. iEEG data were acquired using a 128-channel recording system (Micromed, Treviso, Italy).

B. Preprocessing

First, channels identified as having poor signal quality or containing artifacts during visual inspection are discarded from the raw data. The information about bad channels was already provided on the dataset. Subsequently, a band-stop (notch) filter is applied to eliminate line noise (e.g., 50 Hz). This step aids in reducing interference from electrical sources. Finally, a common average reference is applied to the raw data, wherein EEG channels are re-referenced to the average signal across all channels. This helps mitigate common noise and trends in multiple channels, enhancing the overall data quality for further analysis [7].

C. Brain Connectivity

In the preprocessing of data from fifty-one EEG subjects, functional connectivity (FC) analysis was conducted among the brain regions mentioned in the dataset description. The frequency bands of interest, including alpha (8–13 Hz), theta (4–7 Hz), beta (14–29 Hz), and gamma (30–45 Hz), were further subdivided by 1 Hz increments to capture spectral differences more precisely. For instance, the gamma frequency range was subdivided into 15 segments (30 to 45 Hz) for a detailed exploration of connectivity dynamics. Notably, this approach aimed to uncover nuanced variations within the gamma band.

The MNE-Connectivity library in Python was employed, utilizing the `spectral_connectivity_epochs` function with multitaper frequency estimation [8]. Four distinct calculation methods, Phase Locking Value (PLV), Phase Lag Index (PLI), Pairwise Phase Consistency (PPC), and coherence (COH), were applied to capture diverse aspects of connectivity patterns. PLV uses responses to a repeated stimulus and looks for latencies at which the phase difference between the signals varies little across trials (phase locking) [9]. The Phase Lag Index (PLI) is a connectivity measure designed to capture the asymmetry in the distribution of phase differences between two signals. It emphasizes the presence of non-zero phase lags while disregarding symmetric phase relationships, making it sensitive to directional connectivity [10]. PLI is particularly useful for detecting the presence of uni-directional interactions between brain regions, providing insights into the directed flow of information. Coherence is a measure of functional connectivity that assesses the consistency in the phase relationship between two signals across different frequency components. In essence, it quantifies the degree of synchronization between signals, revealing the strength and stability of their phase coupling. Pairwise Phase Consistency (PPC) is a connectivity metric that assesses the consistency of phase differences across multiple trials by evaluating the similarity in phase relationships across repeated instances of a stimulus or task. PPC provides a measure of the stability of

phase coupling [11]. PPC is the unbiased estimator of the squared PLV.

$$PLV = \left| E \left[\frac{S_{xy}}{|S_{xy}|} \right] \right| \quad (1)$$

$$PLI = \left| E \left[\text{sign} \left(\text{Im}(S_{xy}) \right) \right] \right| \quad (2)$$

$$COH = \frac{|E[S_{xy}]|}{\text{sqrt}(E[S_{xx}] * E[S_{yy}])} \quad (3)$$

$E[\]$ denotes the average over epochs. The connectivity method is based on estimates of the cross- and power-spectral densities (CSD/PSD) S_{xy} and S_{xx}, S_{yy} [8].

$$PPC \equiv \frac{2}{N(N-1)} \sum_{j=1}^{N-1} \sum_{k=(j+1)}^N f(\theta_j, \theta_k) \quad (4)$$

Here, θ_j and θ_k are the relative phases from two observations (j and k are indexing trials or spikes) and f computes the dot product between two-unit vectors [11]. The connectivity is calculated between two channels and assigned a value between 0 and 1, where 0 indicates no connectivity, and 1 signifies the maximum connection. As the connectivity matrix is symmetrical, only the upper triangle of the matrix is utilized to minimize redundancy.

D. Classification

The connectivity matrices obtained from each sub-frequency range were systematically aggregated for every brain wave and calculation method. The resulting stacked matrices were then utilized as input for the classifier, enabling a comprehensive evaluation of classifier performance specific to each brain wave frequency and calculation method. During the preprocessing stage, undesirable channels were identified and discarded, leading to variations in the shapes of resulting brain connectivity matrices. To mitigate this, a zero-padding strategy was employed to homogenize matrix shapes across subjects, ensuring smooth integration for subsequent input into classifiers. Subsequently, for each frequency range (alpha, beta, theta, gamma), the connectivity matrices generated by each method are input into various classifiers, including K-Nearest Neighbors (KNN), Random Forest (RF), Support Vector Machines (SVM), Naive Bayes, Gaussian Process, 2D Convolutional Neural Network (2D CNN), and Multilayer Perceptron (MLP). All classifiers undergo hyperparameter tuning to determine the optimal parameters for maximizing the performance. The hyperparameter tuning process yielded optimal parameter configurations for the classifiers employed in the study. Support Vector Machine (SVM) consistently demonstrated superior performance with a regularization parameter ‘C’ = 100, a radial basis function (RBF) kernel, a polynomial kernel degree of 2, and automatic gamma scaling. Random Forest achieved robust classification using either 200 or 50 as ‘n_estimators’ in different experiments, while

the Gaussian Process maintained stability with a fixed parameter 'n_restarts_optimizer' = 0. Naive Bayes operated with default parameter 'priors' = 'None'. K-Nearest Neighbor (KNN) demonstrated flexibility, achieving optimal results with uniform weights and a 'p' value of 2 in certain instances, along with varying the 'n_neighbors' = (3 or 7) across experiments. The Multilayer Perceptron Network (MLP) configuration was optimized during the hyperparameter tuning process, revealing that the number of layers and neurons could vary. The number of layers did not exceed 3, and the number of neurons remained below 1024. For the 2D Convolutional Neural Network (2D CNN), a single convolution layer with a filter size of (3x3) was consistently employed, and the number of neurons varied between 8 and 256 based on the data. Additionally, a max-pooling layer with dimensions (2,2) was utilized. Binary cross-entropy served as the MLP and CNN's loss function, while the softmax activation function was applied to the output layer.

E. Validation

For the validation of the classification, 80% of the data was used as the training dataset and the remaining 20% as the test set. The classification performance was expressed by classification metrics such as accuracy, precision and recall.

$$Accuracy = \frac{TP + TN}{TP + TN + FP + FN} \quad (5)$$

$$Precision = \frac{TP}{TP + FP} \quad (6)$$

$$Recall = \frac{TP}{TP + FN} \quad (7)$$

Here TP, FP, TN, and FN denote the number of true positives, false positives, true negatives, and false negatives, respectively.

III. RESULTS

Tables I, II, III, IV show the classification metrics corresponding to SVM, RF, GP, NB, KNN, MLP, and CNN classifiers applied to brain connectivity matrices calculated using PLV, PLI, COH, and PPC methods. Notably, SVM demonstrated superior classification performance for both PLV and COH methods in the gamma frequency range. With an accuracy of 97%, and precision and recall reaching 98%, as presented in Table IV, these results surpass the outcomes of previous relevant studies, demonstrating an improvement of 9.64%.

TABLE I. CLASSIFICATION METRICS FOR BRAIN CONNECTIVITY CALCULATION METHODS IN THETA FREQUENCY RANGE

| | | SVM | RF | GP | NB | KNN | MLP | CNN |
|-----|-----------|------|------|------|------|------|------|------|
| PLV | Accuracy | 0.8 | 0.68 | 0.84 | 0.54 | 0.71 | 0.73 | 0.75 |
| | Precision | 0.72 | 0.61 | 0.76 | 0.25 | 0.64 | 0.73 | 0.76 |
| | Recall | 0.89 | 0.71 | 0.91 | 0.03 | 0.8 | 0.73 | 0.76 |
| PLI | Accuracy | 0.76 | 0.84 | 0.75 | 0.54 | 0.58 | 0.84 | 0.78 |
| | Precision | 0.67 | 0.79 | 0.64 | 0.25 | 0.51 | 0.84 | 0.78 |
| | Recall | 0.91 | 0.86 | 1 | 0.03 | 0.97 | 0.84 | 0.78 |
| COH | Accuracy | 0.81 | 0.64 | 0.82 | 0.56 | 0.53 | 0.78 | 0.81 |
| | Precision | 0.74 | 0.56 | 0.73 | 0.33 | 0.47 | 0.78 | 0.82 |
| | Recall | 0.89 | 0.77 | 0.94 | 0.03 | 0.6 | 0.78 | 0.82 |
| PPC | Accuracy | 0.79 | 0.78 | 0.81 | 0.53 | 0.46 | 0.78 | 0.82 |
| | Precision | 0.71 | 0.67 | 0.71 | 0.29 | 0.43 | 0.78 | 0.82 |
| | Recall | 0.86 | 0.97 | 0.97 | 0.06 | 0.83 | 0.78 | 0.82 |

TABLE II. CLASSIFICATION METRICS FOR BRAIN CONNECTIVITY CALCULATION METHODS IN ALPHA FREQUENCY RANGE

| | | SVM | RF | GP | NB | KNN | MLP | CNN |
|-----|-----------|------|------|------|------|------|------|------|
| PLV | Accuracy | 0.77 | 0.67 | 0.86 | 0.49 | 0.73 | 0.74 | 0.74 |
| | Precision | 0.72 | 0.65 | 0.81 | 0.29 | 0.69 | 0.74 | 0.74 |
| | Recall | 0.88 | 0.69 | 0.94 | 0.04 | 0.82 | 0.74 | 0.74 |
| PLI | Accuracy | 0.8 | 0.81 | 0.68 | 0.49 | 0.57 | 0.78 | 0.77 |
| | Precision | 0.73 | 0.74 | 0.61 | 0.29 | 0.53 | 0.78 | 0.77 |
| | Recall | 0.94 | 0.94 | 0.96 | 0.04 | 1 | 0.78 | 0.77 |
| COH | Accuracy | 0.79 | 0.62 | 0.83 | 0.49 | 0.71 | 0.76 | 0.76 |
| | Precision | 0.9 | 0.6 | 0.78 | 0.29 | 0.68 | 0.76 | 0.76 |
| | Recall | 0.87 | 0.69 | 0.92 | 0.04 | 0.78 | 0.76 | 0.76 |
| PPC | Accuracy | 0.79 | 0.72 | 0.79 | 0.49 | 0.62 | 0.73 | 0.81 |
| | Precision | 0.73 | 0.67 | 0.72 | 0.29 | 0.57 | 0.73 | 0.81 |
| | Recall | 0.92 | 0.86 | 0.94 | 0.04 | 0.9 | 0.73 | 0.81 |

TABLE III. CLASSIFICATION METRICS FOR BRAIN CONNECTIVITY CALCULATION METHODS IN BETA FREQUENCY RANGE

| | | SVM | RF | GP | NB | KNN | MLP | CNN |
|-----|-----------|------|------|------|------|------|------|------|
| PLV | Accuracy | 0.94 | 0.78 | 0.96 | 0.48 | 0.92 | 0.82 | 0.91 |
| | Precision | 0.94 | 0.75 | 0.93 | 0.48 | 0.87 | 0.82 | 0.92 |
| | Recall | 0.95 | 0.81 | 1 | 0.48 | 0.99 | 0.82 | 0.92 |
| PLI | Accuracy | 0.79 | 0.94 | 0.75 | 0.5 | 0.61 | 0.75 | 0.96 |
| | Precision | 0.74 | 1 | 0.66 | 0.49 | 0.55 | 0.76 | 0.96 |
| | Recall | 0.87 | 0.89 | 1 | 0.98 | 1 | 0.76 | 0.96 |
| COH | Accuracy | 0.95 | 0.78 | 0.91 | 0.51 | 0.93 | 0.88 | 0.89 |
| | Precision | 0.92 | 0.73 | 0.87 | 0.49 | 0.88 | 0.88 | 0.89 |
| | Recall | 0.98 | 0.87 | 0.96 | 0.94 | 0.94 | 0.88 | 0.89 |
| PPC | Accuracy | 0.87 | 0.83 | 0.87 | 0.48 | 0.76 | 0.84 | 0.89 |
| | Precision | 0.84 | 0.77 | 0.8 | 0.48 | 0.67 | 0.84 | 0.89 |
| | Recall | 0.91 | 0.91 | 1 | 0.98 | 0.99 | 0.84 | 0.89 |

TABLE IV. CLASSIFICATION METRICS FOR BRAIN CONNECTIVITY CALCULATION METHODS IN GAMMA FREQUENCY RANGE

| | | SVM | RF | GP | NB | KNN | MLP | CNN |
|-----|-----------|-------------|------|------|------|------|------|------|
| PLV | Accuracy | 0.97 | 0.81 | 0.96 | 0.52 | 0.91 | 0.9 | 0.92 |
| | Precision | 0.98 | 0.82 | 0.94 | 0.53 | 0.89 | 0.91 | 0.92 |
| | Recall | 0.98 | 0.81 | 1 | 0.93 | 0.97 | 0.91 | 0.92 |
| PLI | Accuracy | 0.83 | 0.91 | 0.76 | 0.53 | 0.67 | 0.82 | 0.85 |
| | Precision | 0.85 | 0.99 | 0.69 | 0.54 | 0.62 | 0.82 | 0.85 |
| | Recall | 0.84 | 0.85 | 1 | 0.93 | 1 | 0.82 | 0.85 |
| COH | Accuracy | 0.97 | 0.83 | 0.94 | 0.52 | 0.95 | 0.93 | 0.93 |
| | Precision | 0.98 | 0.86 | 0.93 | 0.53 | 0.92 | 0.93 | 0.93 |
| | Recall | 0.98 | 0.84 | 0.98 | 0.91 | 0.99 | 0.93 | 0.93 |
| PPC | Accuracy | 0.89 | 0.8 | 0.89 | 0.52 | 0.77 | 0.88 | 0.92 |
| | Precision | 0.93 | 0.83 | 0.84 | 0.53 | 0.71 | 0.89 | 0.92 |
| | Recall | 0.86 | 0.82 | 1 | 0.94 | 0.99 | 0.89 | 0.92 |

We compared classifier performance across PLV, PLI, COH, and PPC methods within various brain wave ranges, employing receiver operating characteristic (ROC) curves and area under the curve (AUC) scores. In Fig. 4, illustrating ROC curves with AUC values for gamma brain waves, SVM exhibited the highest AUC value of 1 for both PLV and COH methods.

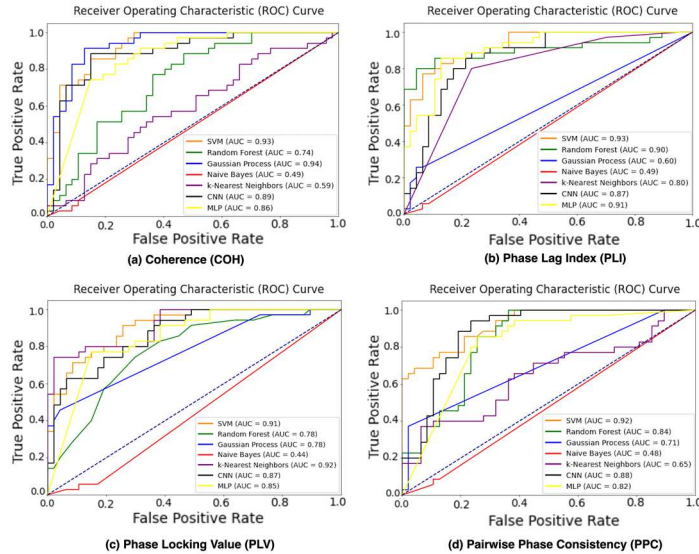


Fig. 1. Theta frequency range's ROC curves with AUC score for testing set for four methods (a) coherence (COH) (b) phase lag index (PLI) (c) phase locking value (PLV) (d) pairwise phase consistency (PPC).

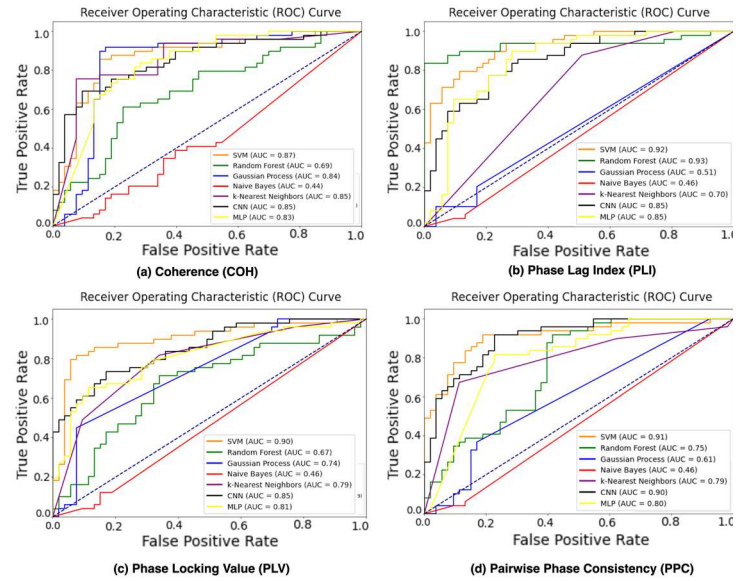


Fig. 2. Alpha frequency range ROC curves with AUC score for testing set for four methods (a) coherence (COH) (b) phase lag index (PLI) (c) phase locking value (PLV) (d) pairwise phase consistency (PPC).

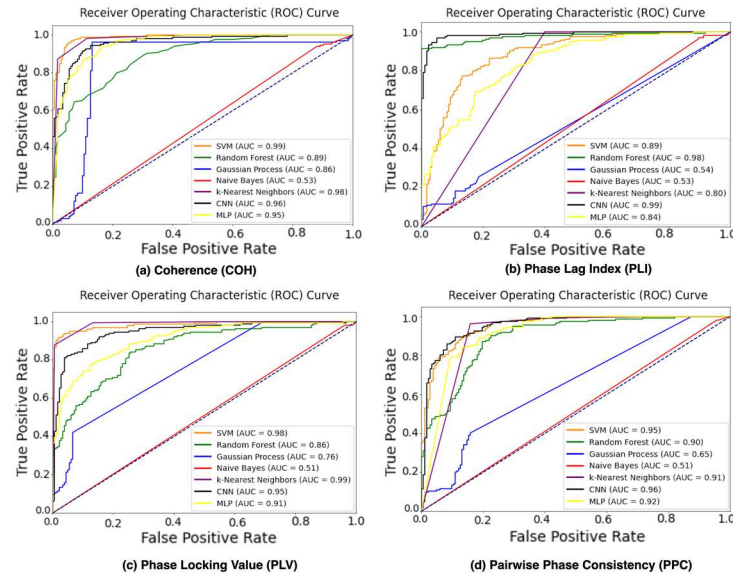


Fig. 3. Beta frequency range's ROC curves with AUC score for testing set for four methods (a) coherence (COH) (b) phase lag index (PLI) (c) phase locking value (PLV) (d) pairwise phase consistency (PPC).

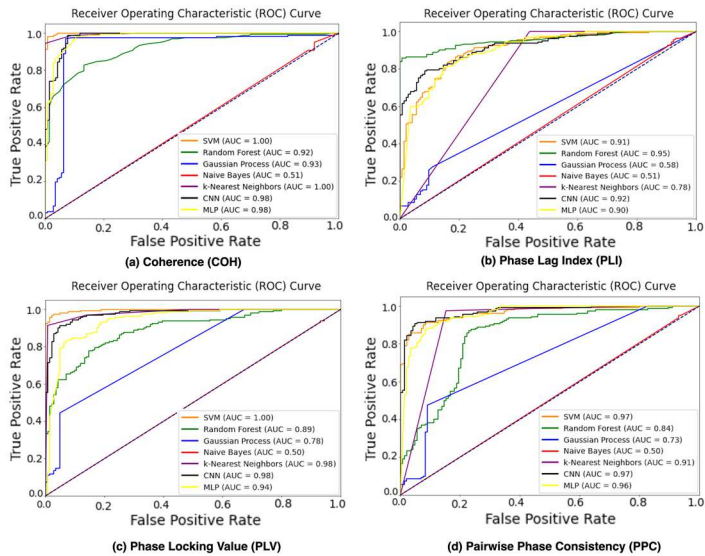


Fig.4. Gamma frequency range’s ROC curves with AUC score for the testing set for four methods (a) coherence (COH) (b) phase lag index (PLI) (c) phase locking value (PLV) (d) pairwise phase consistency (PPC).

IV. DISCUSSION AND CONCLUSION

The study results highlight the significant utility of brain connectivity matrices in effectively classifying closely related auditory stimuli. Notably, the Support Vector Machine (SVM) exhibited superior classification accuracy, although it necessitated meticulous hyperparameter tuning. The deep learning classifier, exemplified by the CNN, demonstrated secondary performance, even though it was designed with a simple architecture—specifically, one convolution layer with a reduced number of neurons. However, the training time was significantly higher even with Google Colab GPU compared to traditional machine learning algorithms. Despite the advantageous feature extraction capabilities of deep learning classifiers, this research underscores that traditional machine learning methods, such as SVM, can adeptly handle connectivity information from two channels, achieving superior classification metrics. Moreover, classification accuracy was notably higher for faster brain waves, like gamma, compared to slower brain waves, such as alpha and theta. The choice of brain connectivity calculation methods also played a pivotal role, with Phase Locking Value (PLV) and Coherence (COH) proving more effective in achieving accuracy with classifiers compared to Phase Lag Index (PLI) and Pairwise Phase Consistency (PPC). In conclusion, this research not only tested but also validated the viability of utilizing brain connectivity matrices for auditory-based BCI. It delves into the influential factors of brain waves and connectivity calculation methods in the classification process. The outcomes of this study offer valuable insights for designing auditory BCIs and advancing research in reconstructing music or speech from neural activity, contributing to a deeper understanding of the associated cognitive processing.

REFERENCES

[1] J. Cao *et al.*, “Brain functional and effective connectivity based on electroencephalography recordings: A review,” *Human Brain*

Mapping, vol. 43, no. 2. John Wiley and Sons Inc, pp. 860–879, Feb. 01, 2022. doi: 10.1002/hbm.25683.

[2] Y. Huang and C. Keller, “How can I investigate causal brain networks with iEEG?” arXiv, 2022. doi: 10.48550/arXiv.2205.07045.

[3] J. Carmenta, P. Sajda, Institute of Electrical and Electronics Engineers, and IEEE Engineering in Medicine and Biology Society, *9th International IEEE EMBS Conference on Neural Engineering: 20-23 March 2019, the Hilton Union Square, San Francisco, California*.

[4] S. E. Moon, C. J. Chen, C. J. Hsieh, J. L. Wang, and J. S. Lee, “Emotional EEG classification using connectivity features and convolutional neural networks,” *Neural Networks*, vol. 132, pp. 96–107, Dec. 2020, doi: 10.1016/j.neunet.2020.08.009.

[5] S. Jang, S. Moon, and J.-S. Lee, “Eeg-Based Video Identification Using Graph Signal Modeling and Graph Convolutional Neural Network,” *2018 IEEE International Conference on Acoustics, Speech and Signal Processing (ICASSP)*, pp. 3066–3070, 2018, [Online]. Available: <https://api.semanticscholar.org/CorpusID:52196003>

[6] J. Bereztuskaya *et al.*, “Open multimodal iEEG-fMRI dataset from naturalistic stimulation with a short audiovisual film,” *Sci Data*, vol. 9, no. 1, Dec. 2022, doi: 10.1038/s41597-022-01173-0.

[7] D. Yao, Y. Qin, S. Hu, L. Dong, M. L. Bringas Vega, and P. A. Valdés Sosa, “Which Reference Should We Use for EEG and ERP practice?,” *Brain Topography*, vol. 32, no. 4. Springer New York LLC, pp. 530–549, Jul. 30, 2019. doi: 10.1007/s10548-019-00707-x.

[8] A. Gramfort *et al.*, “MEG and EEG data analysis with MNE-Python,” *Front Neurosci*, no. 7 DEC, 2013, doi: 10.3389/fnins.2013.00267.

[9] J.-P. Lachaux, E. Rodriguez, J. Martinerie, and F. J. Varela, “Measuring Phase Synchrony in Brain Signals,” 1999.

[10] C. J. Stam, G. Nolte, and A. Daffertshofer, “Phase lag index: Assessment of functional connectivity from multi channel EEG and MEG with diminished bias from common sources,” *Hum Brain Mapp*, vol. 28, no. 11, pp. 1178–1193, Nov. 2007, doi: 10.1002/hbm.20346.

[11] M. Vinck, M. van Wingerden, T. Womelsdorf, P. Fries, and C. M. A. Pennartz, “The pairwise phase consistency: A bias-free measure of rhythmic neuronal synchronization,” *Neuroimage*, vol. 51, no. 1, pp. 112–122, 2010, doi: 10.1016/j.neuroimage.2010.01.073.